BBA - Molecular Basis of Disease 1870 (2024) 166857

Contents lists available at ScienceDirect

BBA - Molecular Basis of Disease

journal homepage: www.elsevier.com/locate/bbadis

Amyloid pathology reduces ELP3 expression and tRNA modifications leading to impaired proteostasis

Marisa Pereira [a], Diana R. Ribeiro [a], Maximilian Berg [b], Andy P. Tsai [c], Chuanpeng Dong [d], Kwangsik Nho [e], Stefanie Kaiser [b], Miguel Moutinho [e], Ana R. Soares [a,*]

[a] Institute of Biomedicine (iBiMED), Department of Medical Sciences, University of Aveiro, Aveiro, Portugal
[b] Institute of Pharmaceutical Chemistry, Goethe-University, Frankfurt, 60438, Germany
[c] Wu Tsai Neurosciences Institute, Stanford University School of Medicine, Stanford, CA, USA
[d] Department of Medical and Molecular Genetics, Center for Computational Biology and Bioinformatics, Indiana University School of Medicine, Indianapolis, IN, USA
[e] Stark Neurosciences Research Institute, Indiana University School of Medicine, Indianapolis, IN, USA

ARTICLE INFO

Keywords:
Alzheimer's disease
Elongator complex subunit 3 (ELP3)
Proteostasis
Translation
tRNA modifications

ABSTRACT

Alzheimer's Disease (AD) is a neurodegenerative disorder characterized by accumulation of β-amyloid aggregates and loss of proteostasis. Transfer RNA (tRNA) modifications play a crucial role in maintaining proteostasis, but their impact in AD remains unclear. Here, we report that expression of the tRNA modifying enzyme *ELP3* is reduced in the brain of AD patients and amyloid mouse models and negatively correlates with amyloid plaque mean density. We further show that SH-SY5Y neuronal cells carrying the amyloidogenic *Swedish* familial AD mutation (SH-SWE) display reduced ELP3 levels, tRNA hypomodifications and proteostasis impairments when compared to cells not carrying the mutation (SH-WT). Additionally, exposing SH-WT cells to the secretome of SH-SWE cells led to reduced ELP3 expression, wobble uridine tRNA hypomodification, and increased protein aggregation. Importantly, correcting tRNA deficits due to ELP3 reduction reverted proteostasis impairments. These findings suggest that amyloid pathology dysregulates proteostasis by reducing ELP3 expression and tRNA modification levels, and that targeting tRNA modifications may be a potential therapeutic avenue to restore neuronal proteostasis in AD and preserve neuronal function.

1. Introduction

Alzheimer's disease (AD) is a progressive neurodegenerative disorder and the leading cause of dementia in the elderly [3]. It is often characterized by early memory impairment and progressive cognitive decline that results from synapse loss and neuronal atrophy predominately throughout the hippocampus and cerebral cortex [60]. Pathologically, AD is characterized by an abnormal accumulation of protein aggregates, namely extracellular deposition of amyloid-β (Aβ) peptides in senile plaques and the intracellular accumulation of hyperphosphorylated tau (P-tau) that forms neurofibrillary tangles, followed by neurodegeneration [13,60]. Despite the underlying mechanisms are still largely unknown, mounting evidence suggests that the accumulation and aggregation of Aβ is a key initiating factor in a cascade of events that lead to this disorder, which include P-tau tangles and neuronal loss [58]. There are also reports indicating that the dissemination of Aβ and P-tau by small extracellular vesicles or exosomes further promotes neurodegeneration [49,56], and cognitive impairment in AD that has been associated with dysregulation of RNA and protein expression profiles in the brain [42].

Dysregulation of protein translation is emerging as a central mechanism in the pathogenesis of neurodegenerative disorders [20,23,32,37,66]. Neurons are particularly dependent on spatial and temporal control of mRNA translation, and disruptions in translation components have a dramatic impact on neuronal survival [66]. One of these components are transfer RNAs (tRNAs) [50], that recognize mRNA codons through their anticodons to decode the 20 standard amino acids, linking the genetic code information to amino acid identity [46]. To be fully active, tRNAs undergo extensive post-transcriptional modifications, catalyzed by different tRNA modifying enzymes [47]. From all RNA molecules, tRNAs are the most chemically modified class, with an average of 13 modifications per tRNA, that are collectively known as the tRNA epitranscriptome [46]. These post-transcriptional chemical modifications are pivotal for tRNA stability and translation efficiency and

* Corresponding author.
E-mail address: ana.r.soares@ua.pt (A.R. Soares).

https://doi.org/10.1016/j.bbadis.2023.166857
Received 15 May 2023; Received in revised form 9 August 2023; Accepted 22 August 2023
Available online 26 August 2023

fidelity [46,47]. Modifications occurring outside the anticodon loop of tRNAs are crucial for tRNA stability and recognition by amino-acyltransferases. On the other hand, modifications that occur at the anticodon loop, particularly at the wobble position, ensure the diversity of codon recognition and translation efficiency as they optimize mRNA decoding, and improve or stabilize codon-anticodon interactions, contributing to maintain proteome integrity by counteracting protein aggregation [46,50]. Disruptions in tRNA modifications have a direct impact on tRNA expression, mRNA decoding and protein translation, leading to pathological conditions known as "tRNA modopathies" [10].

Growing evidence shows that the human brain is particularly sensitive to tRNA epitranscriptome defects [5]. tRNA modifications, particularly the ones at the anticodon, and their corresponding tRNA modifying enzymes, have been implicated in a panoply of neurological diseases [47], namely intellectual disability [2,12,30,35,39], familial dysautonomia [4,27,33,72], and motor neuron diseases such as amyotrophic lateral sclerosis (ALS) [7,61]. In general terms, disruption of tRNA modifying enzymes occur in these diseases, affecting the levels of tRNA modifications and leading to defects in mRNA translation in a codon-dependent manner. Quite surprisingly, the impact of tRNA modifications and related networks in AD pathophysiology has been poorly explored and characterized. However, there are indications showing that the tRNA epitranscriptome may represent an AD modifier. For example, a recent report showed m^1A tRNA hypomodification and decreased expression of the corresponding tRNA modifying enzyme in the AD amyloidogenic 5xFAD mouse model [59], and NSUN2, a methyltransferase that methylates cytosine to 5-methylcytosine (m^5C) in tRNAs, was found downregulated in the hippocampus of early onset AD patients [71]. Also, global reduction of protein synthesis rate and increased levels of phosphorylated eIF2α (eIF2α—P) have been found in the cortex and hippocampus of AD patients and mouse models [36,62,68], similarly to what we have observed when inducing tRNA mutations or tRNA hypomodification in vertebrates and in human cell lines [48,54,67], further re-enforcing the relevance of tRNA molecules and their modifications in the AD context. Compelled by these clues, we hypothesized that dysregulation of tRNA modifying enzymes and, consequently, of tRNA modifications occurs in AD and lead to neuronal proteostasis impairment.

Here, we report that *ELP3* expression is reduced in the brain tissue of AD patients and of amyloidogenic 5xFAD mice, and in neuronal cell models expressing the *Swedish* familial AD mutation. Our results suggest that amyloid pathology reduces *ELP3* expression and consequently leads to tRNA hypomodification, proteostasis impairments and toxicity in neuronal cells. Importantly, we provide evidence that correction of tRNA deficits incurring from *ELP3* deficiency rescues proteostasis, reinforcing that tRNAs and tRNA modifications are essential to maintain protein homeostasis in AD and that the tRNA epitranscriptome can represent a promising therapeutic target.

2. Results

2.1. ELP3 is differentially expressed in AD patients and its abundance negatively correlates with amyloid plaque density

To evaluate the expression of tRNA modifying enzymes across different human brain regions we used harmonized RNA-seq data generated from three cohort studies, namely, Religious Orders Study and Memory and Aging Project (ROSMAP), Mount Sinai Brain Bank (MSBB), and Mayo RNA-seq (Mayo) available online at *https://agora.adknowledgeportal.org/ [19]*. We assessed the gene expression of 56 known tRNA modifying enzymes in the different brain regions available on these datasets and found that several were significantly differential expressed (S_Table 1). From those, the majority was negatively differentially expressed between AD cases and controls in at least one brain region, particularly the tRNA modifying enzymes that catalyze modifications at the wobble position (Table 1).

Among these we identified *NSUN2,* whose expression was previously found decreased in the hippocampus of early onset AD patients [71]. *ADAT2* and *ADAT3*, that catalyze wobble adenosine-to-inosine (A-to-I) modifications, were the 2 enzymes displaying the highest differentially expression, but in a compensatory manner. Whenever *ADAT2* was negatively differentially expressed, *ADAT3* was positively differentially expressed in a similar magnitude for most of the tissues assessed. Consistently, tRNA modifying enzymes that catalyze wobble uridine modifications and belong to the Elongator complex, namely *ELP1*, *ELP3,* and *ELP6,* were negatively differentially expressed in the Parahippocampal Gyrus (PHG), one of the most affected brain regions in AD. *ALKBH8*, the methyltransferase that catalyzes the subsequent mcm^5U_{34}

Table 1
Visual representation of the significant differentially expressed tRNA modifying enzymes that catalyze modifications at the wobble position, in different brain areas of Alzheimer's disease patients, compared to cognitively normal older adults. Note that red bars indicate negative differential expression levels and green bars indicates positive differential expression values (p-value <0.05). Values range from −4.3E-01 (lowest) to 3.9E-01 (highest). Abbreviations: tRNA modifying enzymes (tRNAModEnz).

tRNAModEnz	Anterior Cingulate Cortex	Cerebellum	Dorsolateral Prefrontal Cortex	Frontal Pole	Inferior Frontal Gyrus	Posterior Cingulate Cortex	Parahippocampal Gyrus	Superior Temporal Gyrus	Temporal Cortex
IKBKAP/ELP1									
ELP2									
ELP3									
ELP4									
ELP5									
ELP6									
URM1									
CTU1									
CTU2									
ALKBH8									
FTSJ1									
QTRT1									
NSUN2									
TRMU									
ADAT2									
ADAT3									
NSUN3									
GTPBP3									
TRDMT1									

modification that follows the cm^5U_{34} modification catalyzed by the Elongator complex, was also found negatively differentially expressed in different brain regions, including the PHG.

To elucidate potential connections between the dysregulation of these tRNA modifying enzymes and specific AD characteristics, we investigated possible correlations with amyloid plaque burden. We found a significant negative correlation between *ELP3* expression levels and amyloid plaque burden in the PHG ($\beta = -0.006$, $p = 3.75E\text{-}03$) (Fig. 1) using data extracted from the MSBB cohort [70]. However, no correlations were observed between any of the other dysregulated Elongator complex proteins, namely *ELP1* and *ELP6*, nor with *ALKBH8*, which acts after the Elongator complex on wobble uridines of specific tRNAs (Fig. 1). To further confirm if this negative correlation was specific for *ELP3*, we extended the analysis to additional tRNA modifying enzymes that display similar disruption to *ELP3*, and that catalyze other wobble modifications, namely *FTSJ1 and ADAT2*. No correlation

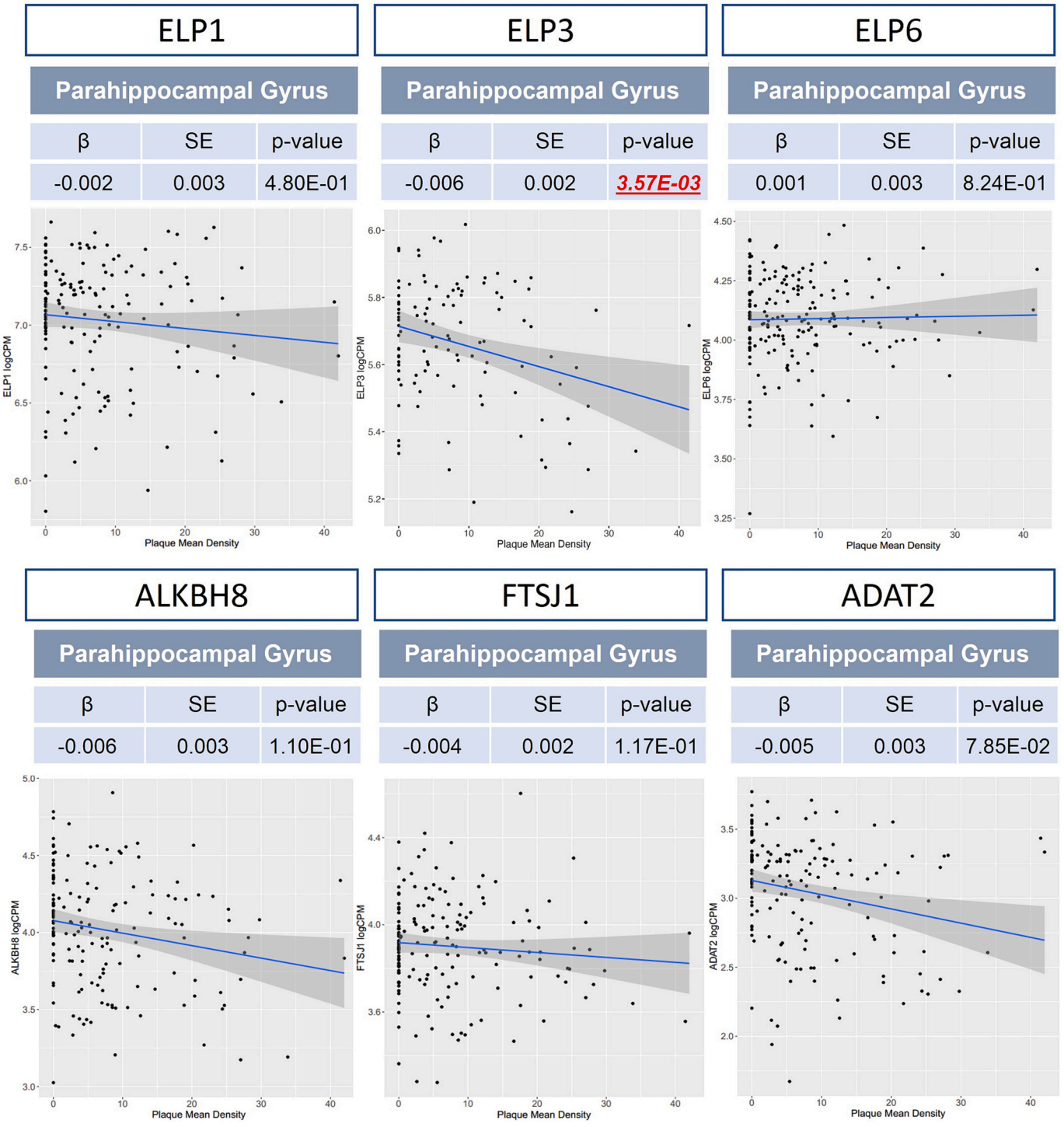

Fig. 1. Correlation analysis between expression levels of *ELP1, ELP3, ELP6, ALKBH8, FTSJ1* and *ADAT2* and amyloid plaque mean density (number of plaques/mm^2) in the PHG. The scatter plots only show a significant negative association between *ELP3* expression and plaque mean density in the PHG region ($\beta = -0.006$, *p*-value = 3.52E-03). Data extracted from the MSBB cohort [70]. In the study, the β coefficient (β) represents the effect size, while the standard error (SE) measures the precision of the estimate. Abbreviations: β coefficient (β) and standard error (SE).

between any of these enzymes and amyloid plaque burden was found (Fig. 1). We have also tried to perform the same correlation analysis for *ADAT3*, but due to the low expression levels reported in the MSBB cohort, this calculation was not possible.

These findings were further complemented with a subsequent convergent functional genomic (CFG) analysis, which aimed to prioritize AD candidate genes using the AlzData datasets (http://www.alzdata.org/). The results indicated that among the differentially expressed tRNA modifying enzymes in AD patients, *ELP3* was the only one that cumulative revealed a significant negative correlation between its expression with amyloid and tau pathology based on different amyloidogenic (APPK670N/M671L and PSEN1 M146V mutations) and tauopathy (MAPT P301L mutation) murine models (S_Table 2; Table 2), and that was identified as an early differential expressed gene, retrieving the highest CFG score (4 out of 5) for the tRNA modifying enzymes analyzed.

Collectively, this data pointed towards the importance of *ELP3* in amyloid pathology, which led us to focus on this enzyme and its tRNA catalyzed modifications for the subsequent studies.

2.2. ELP3 expression and its dependent tRNA modifications are decreased in the hippocampus of 5xFAD mice

Since our patient and animal AD model dataset analysis identified *ELP3* as an early differential expressed gene, we decided to validate this finding in the hippocampus of the amyloid mouse model 5xFAD, that expresses five human familial AD mutations. This model depicts $A\beta_{1-42}$ overproduction, widespread plaque deposition, alterations in immune-related genes, neuronal loss and cognitive decline [43]. We analyzed *ELP3* mRNA expression in the hippocampus of 1-month-old (1 M), 4 M and 8 M 5xFAD mice and C57BL/6 J controls (B6) (Fig. 2A). We observed a statistically significant decrease of *ELP3* mRNA (~15 % decrease) and protein expression (~40 % decrease) only in the hippocampus of 4 M 5xFAD mice (Fig. 2B,C), a stage that coincides with learning and memory deficits when amyloid plaques and astrogliosis is increased, which are hallmarks of the prodromal stage of AD, that precedes irreversible degeneration [18].

The Elongator complex and its catalytical subunit ELP3 are essential for cm^5U catalysis that precedes the mcm^5U and the final mcm^5s^2U modification at the wobble position of three specific tRNAs: tRNA-Glu^{UUC}, tRNA-Gln^{UUG} and tRNA-Lys^{UUU} [1]. Upon quantification of tRNA modification levels by liquid-chromatography coupled with tandem mass spectrometry (LC-MS/MS), both mcm^5U and mcm^5s^2U modifications were significantly decreased in the hippocampus of 4 M 5xFAD mice in comparison to control mice (Fig. 2D). Levels of the other tRNA modifications assessed were not significantly affected, except for the inosine (I) modification, whose levels were increased in the hippocampus of 4 M 5xFAD mice (Suppl. Fig. 1).

2.3. ELP3 abundance is decreased in cellular models bearing the familial AD Swedish mutation

According to the Human Protein Atlas (www.proteinatlas.org), *ELP3* is expressed at higher levels in neuronal cells than in glial cells in brain tissue, which is consistent with observations in mice [7]. To further understand the implications of *ELP3* differential abundance in the context of AD, we performed different *in vitro* experiments using human neuroblastoma cells (SH-SY5Y) stably expressing either wild-type amyloid precursor protein (APP) (from now on referred to as SH-WT), or the APP695 mutation, a familial AD mutation, also known as the *Swedish* mutation (from now on referred to as SH-SWE) [17,63]. This APP695 mutation occurs at the β-secretase cleavage site, resulting in the production and deposition of toxic amyloid-β (Aβ) forms (Fig. 3A) and is also one of the familial AD mutations present in the 5xFAD mice used in this study. Western blotting of APP confirmed its high expression on the SH-WT and SH-SWE cell lines when compared to the original SH-SY5Y cell line, as expected (Fig. 3A), and no differences on cell viability were found between SH-WT and SH-SWE cells (Fig. 3B).

ELP3 mRNA and protein expression was significantly decreased in SH-SWE cells compared to SH-WT cells, by approximately 26 % and 57 %, respectively (Fig. 3C, D). These values were in line with ELP3 mRNA and protein expression disruption observed in the hippocampus tissue of 4 M 5xFAD mice in comparison with controls (Fig. 2B, C). Additionally, the expression of ELP3 was maintained between the undifferentiated and differentiated state in both SH-SWE and SH-WT cell lines (Suppl. Fig. 2A), suggesting that the levels of ELP3 do not change with differentiation, but change in the presence of the familial SWE mutation. SH-SWE cells were also characterized by significant accumulation of

Table 2
Convergent functional genomic (CFG) analysis for target genes. The *ELP3* gene is highlighted in red. Information collected from http://www.alzdata.org/ [1]. Abbreviations: expression quantitative trait loci (eQTL); genome-wide association studies (GWAS); protein-protein interaction (PPI), and differentially expressed genes (DEG).

Gene	eQTL	GWAS	PPI	Early_DEG	Pathology cor (abeta)	Pathology cor (tau)	CFG
IKBKAP/ELP1	1	0	–	yes	−0.391,**	−0.088,ns	3
ELP2	2	0	–	NA	NA	NA	1
ELP3	1	1	–	yes	−0.456,**	−0.602,*	4
ELP4	3	0	–	NA	NA	NA	1
ELP5	NA	0	–	NA	NA	NA	0
ELP6	NA	0	–	NA	NA	NA	0
URM1	2	NA	–	NA	NA	NA	1
CTU1	0	0	–	NA	NA	NA	0
CTU2	0	0	–	NA	NA	NA	0
ALKBH8	0	3	–	NA	NA	NA	1
FTSJ1	1	NA	–	NA	NA	NA	1
QTRT1	0	0	–	yes	−0.173,ns	0.261,ns	1
NSUN2	0	0	–	NA	−0.093,ns	−0.427,ns	0
TRMU	1	0	–	NA	NA	NA	1
ADAT2	0	0	–	NA	NA	NA	0
ADAT3	6	0	–	NA	NA	NA	1
NSUN3	1	0	–	NA	−0.055,ns	−0.102,ns	1
GTPBP3	0	0	–	NA	0.079,ns	−0.405,ns	0
TRDMT1	3	0	–	NA	NA	NA	1

[1] This note outlines the different criteria used to evaluate the significance of a target gene's role in AD. These include eQTL analysis to examine genetic regulation, GWAS studies, PPI analysis to identify physical interactions (APP, PSEN1, PSEN2, APOE or MAPT), identification as an early-DEG, and correlation with AD pathology (abeta and tau) in AD mouse models. The significance level is determined by *p*-values, with * indicating $p < 0.05$ and ** indicating $p < 0.01$. The CFG score is a cumulative score that ranges from 0 to 5 and is based on the presence or absence of significant evidence across these criteria.

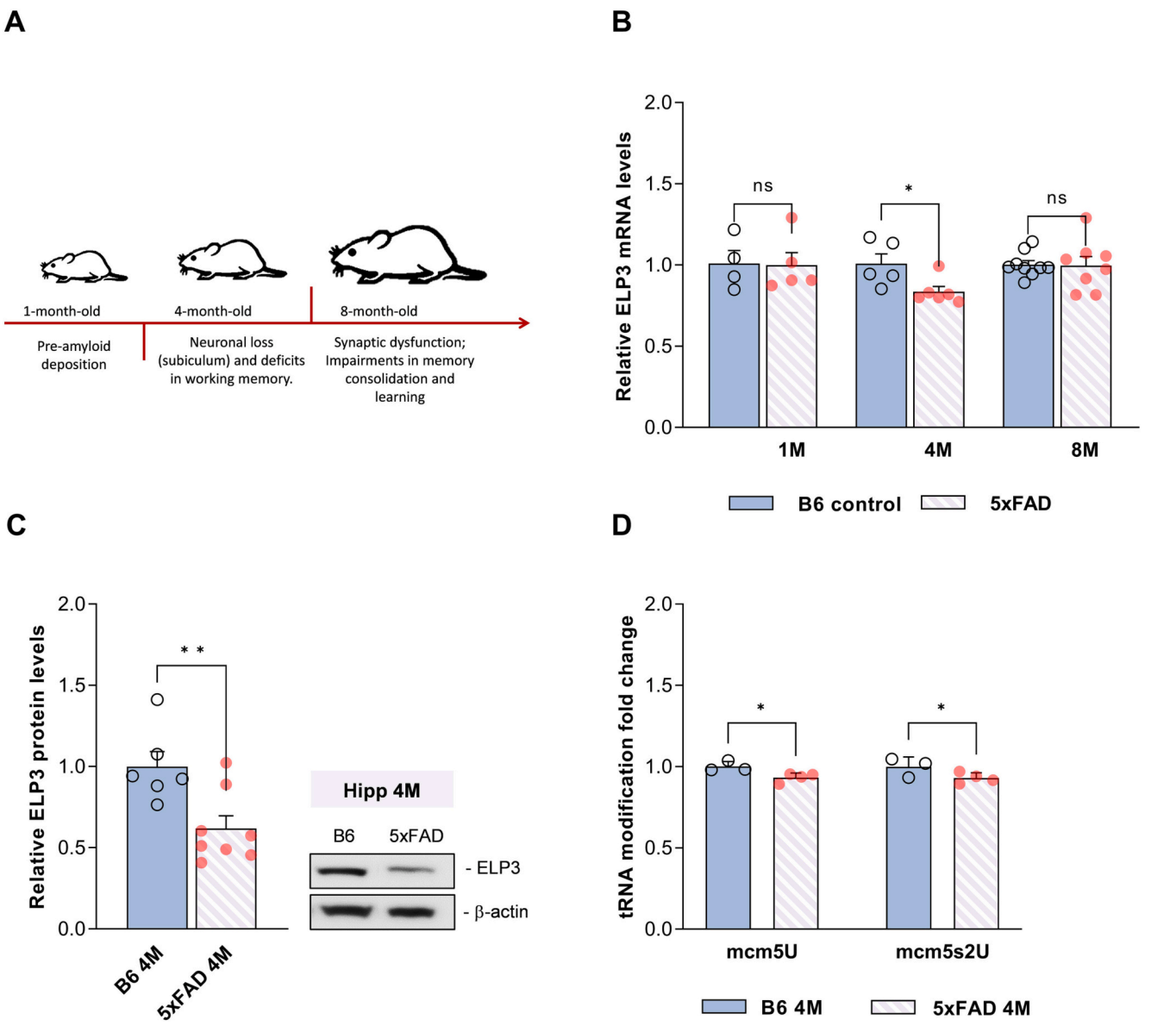

Fig. 2. ELP3 is less abundant in the hippocampus (Hipp) of 4-month-old (4 M) 5xFAD mice. A) Schematic representation of the primary pathological alterations in 5xFAD mice at 1 M, 4 M and 8 M. B) qPCR analysis of ELP3 mRNA levels in the Hipp of 5xFAD and non-transgenic control (B6) animals, at 1 M (*n 5xFAD* = 5 males; *n B6* = 4 males), 4 M (*n 5XFAD* = 5 males +1 female; *n B6* = 3 males +2 females), and 8 M (*n 5xFAD* = 8 females; *n B6* = 9 females). *ELP3* mRNA levels were significantly decreased in the Hipp of 5xFAD mice at 4 M when compared to the control B6 mice. GAPDH was used as a housekeeping gene. C) Western blot and graphical representation of ELP3 protein levels in the Hipp of 4 M 5xFAD ($n = 8$ females) and non-transgenic control (B6) ($n = 6$ females) animals. ELP3 protein levels were significantly decreased in the Hipp of 5xFAD at 4 M compared to control B6 mice. β-actin was used as an internal control. D) Quantification of the wobble tRNA modifications in the Hipp of 5xFAD and non-transgenic control (B6) animals at 4 M (*n 5xFAD* = 3 males +1 female; *n B6* = 2 males +1 female). A significant decrease in the levels of mcm^5U and mcm^5s^2U modifications was detected in the Hipp of 5xFAD at 4 M compared to control B6 mice. Data information: data are expressed as mean with SEM. *p-value <0.05, **p-value <0.01 and non-significant (ns) p-value as assessed by unpaired t-test (in B—D).

insoluble proteins (Fig. 3E) and impaired protein synthesis, as detected by the puromycin incorporation assay SUnSET [57] (Fig. 3F), and increased eIF2α-P (Fig. 3G). This was expected since APP695 mutation leads to deposition of toxic Aβ forms and decreased ELP3 levels are associated with translation impairments through increased levels of eIF2α-P and accumulation of protein aggregates as demonstrated by us and others [14,51,64].

The lower expression of ELP3 in SH-SWE cells was also accompanied by a significant decrease in mcm^5U levels, but not in mcm^5s^2U levels (Fig. 4A). As this was unexpected, we analyze the thiolation levels of tRNA-Lys^{UUU}, one of the 3 tRNAs that carries the final mcm^5s^2U modification, by an alternative method that consists on an APM gel electrophoresis, combined with Northern blotting for the tRNA of interest [22,34]. 2-thiolated (s^2) tRNAs migrate more slowly compared to non-thiolated tRNAs in the APM gel, which allows to conclude on the amount of tRNA that is 2-thiolated. Although quantification of mcm^5s^2U levels in total tRNA by LC/MS-MS did not reflect any alteration between cell lines, we observed a significant decrease in the amount of 2-thiolated tRNAs-Lys^{UUU} in the SH-SWE cells when compared with SH-WT cells (Fig. 4B). As a control, we used the tRNA-Ser^{AGA}, that is not modified by the Elongator complex, neither undergoes 2-thiolation (Fig. 4C). Although tRNA-Lys^{UUU} was significantly decreased in SH-SWE cells, decreased s^2 was not due to a decrease in the tRNA absolute expression as data was normalized for the internal control 5S and for the tRNA-Lys^{UUU} quantity detected by regular Northern blotting (Fig. 4D). No differences were detected in any of the other modifications

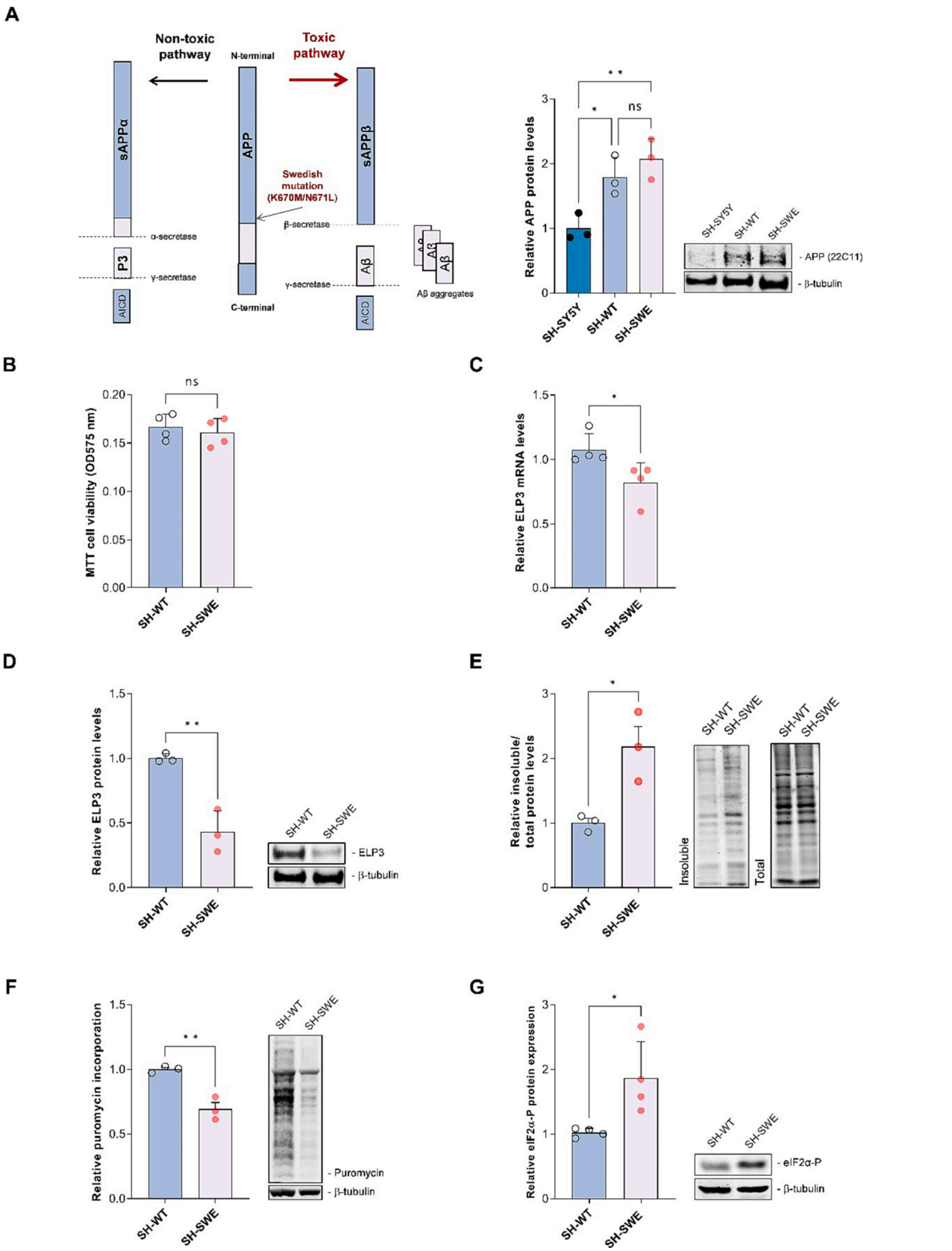

(caption on next page)

Fig. 3. SH-SWE cells are characterized by ELP3 decreased expression, increased levels of insoluble proteins and impaired protein synthesis. A) Schematic representation of the *Swedish* mutation in the β-site of APP, which shifts APP processing towards the toxic pathway due to an increase in Aβ production. Western blot and graphical representation of APP protein levels in SH-SY5Y, SH-WT and SH-SWE cells. A significant increase in APP expression was observed in both SH-WT and SH-SWE cells compared to SH-SY5Y cells. β-tubulin was used as an internal control. B) MTT assay to test cellular viability. No significant alterations in the cellular viability were found in SH-SWE cells compared to SH-WT cells. C) Quantification of ELP3 mRNA levels by qPCR. A significant decrease in the expression of ELP3 was observed in SH-SWE cells when compared to SH-WT cells. GAPDH was used as a housekeeping gene. D) Quantification of ELP3 protein levels by Western blotting. A significant decrease in the expression of ELP3 was observed in SH-SWE cells when compared to SH-WT cells. β-tubulin was used as an internal control. E) Quantification of relative insoluble protein fraction. A significant increase in the amount of insoluble protein levels was observed in SH-SWE cells compared to SH-WT cells. Representative acrylamide gels of both insoluble and total fractions after blue safe staining are depicted. F) Relative rate of protein synthesis based on the incorporation of puromycin by the SUnSET method. A significant decrease in puromycin incorporation during translation was observed in SH-SWE cells compared to SH-WT cells by Western blotting. β-tubulin was used as an internal control. G) Quantification of eIF2α-P expression by Western blotting. A significant increase in eIF2α-P was observed in SH-SWE cells compared to SH-WT cells. β-tubulin was used as an internal control. Data information: data are expressed as mean with SEM, with at least a $n = 3$ biological replicates. *p-value <0.05, **p-value <0.01, and non-significant (ns) p-value as assessed by one way ANOVA (in A) and unpaired t-test (B-G).

analyzed (Suppl. Fig. 2B).

As it is well established that ELP3 and the Elongator complex participates in the final mcm^5s^2U modification of 2 other tRNAs, namely tRNA-Glu^{UUC} and tRNA-Gln^{UUG} and that tRNA hypomodification may impact tRNA abundance [55], we have also quantified the expression of the mentioned tRNAs by Northern blotting. Our data shows that, similarly, to tRNA-Lys^{UUU}, tRNA-Glu^{UUC} is significantly decreased in SH-SWE cells (Suppl. Fig. 2C), but no difference was detected in tRNA-Gln^{UUG} (Suppl. Fig. 2D), nor in tRNA-Ser^{AGA}, which was used as a control (Fig. 4E). Despite that, we found a decrease in s^2 levels of both tRNA-Glu^{UUC} and tRNA-Gln^{UUG} in SH-SWE cells (Suppl. Fig. 2E, F), and no thiolated tRNA-Ser^{AGA} was detected in any of the cell lines, as expected (Fig. 4C). These results indicate that the reduction in s^2 is not limited to tRNA-Lys^{UUU} but extends to the other tRNAs that also carry the final mcm^5s^2U modification.

We then performed additional experiments where we induced alterations in the expression levels of ELP3 and/or of tRNA-Lys^{UUU} abundance. Efficient *ELP3* silencing was achieved in both SH-WT and SH-SWE cells, with a silencing efficiency of ~70 % in both cell lines at the mRNA and protein level (Fig. 5A, B). Silencing of *ELP3* expression in SH-WT cells mimicked the accumulation of insoluble proteins that occurs in SH-SWE cells (Fig. 5C) and negatively affected tRNA-Lys^{UUU} expression (Fig. 5D). Silencing of *ELP3* did not have an impact on the abundance of tRNA-Ser^{AGA} in either of the cell lines as expected, as this tRNA is not modified by the Elongator complex (Fig. 5E).

Efficient transfection of a plasmid encoding an unmodified tRNA-Lys^{UUU} resulted in a significant increase of tRNA-Lys^{UUU} abundance in both SH-WT cells and SH-SWE cells, regardless of prior *ELP3* silencing (Suppl. Fig. 3). Overexpression of the unmodified tRNA-Lys^{UUU} in *ELP3* silenced SH-WT (SH-WT siELP3 + tRNA-Lys condition – Fig. 5C) was sufficient to revert the accumulation of insoluble proteins to SH-WT basal levels (SH-WT siCTRL + tRNA-Mock condition – Fig. 5C). No alterations were observed at the proteostasis level when we overexpressed the tRNA-Lys^{UUU} in SH-WT cells that were not previously *ELP3*-silenced (SH-WT siCTRL + tRNA-Lys condition – Fig. 5C). However, as expected, transfection of the tRNA-Lys^{UUU} plasmid in SH-SWE cells (SH-SWE siCTRL + tRNA-Lys and SH-SWE siELP3 + tRNA-Lys conditions – Fig. 5C) restored proteostasis by decreasing the accumulation of insoluble proteins characteristic of SH-SWE (SH-SWE siCTRL+ tRNA-Mock and SH-SWE siELP3 + tRNA-Mock conditions – Fig. 5C) and reverted its levels to SH-WT insoluble protein fraction levels (SH-WT siCTRL+ tRNA-Mock condition – Fig. 5C), independently of previous transfection of these cells with an siRNA against *ELP3*. Together, this data shows that overexpressing an unmodified tRNA in tRNA hypomodification conditions, namely upon *ELP3* silencing, counteracts the lack of modifications.

2.4. The secretome of SH-SWE cells negatively affects ELP3 abundance and tRNA modification levels and increases the accumulation of insoluble proteins in SH-WT cells

Since SH-SWE cells are characterized by a specific APP mutation that induces the accumulation of toxic Aβ forms, we wondered if the observed disruption in ELP3 abundance occurred in response to the proteotoxic stress that is already triggered by the mutation. To elucidate if this was the case, we evaluated the effects produced by the SH-SWE secretome, that includes the secreted toxic Aβ forms, on SH-WT cells. Upon 72 h incubation of SH-WT with SH-SWE secretome, ELP3 expression was decreased by ~30 % when compared with SH-WT cells incubated with their own secretome (Fig. 6A). These cells recapitulated all SH-SWE findings reported above (Fig. 3). There was a significant increase (90 % increase) in accumulation of cellular insoluble proteins (Fig. 6B), and a decrease in protein synthesis of approximately 15 % (Fig. 6C). Additionally, mcm^5U modification levels were negatively impacted in SH-WT cells incubated with SH-SWE secretome as quantified by LC-MS/MS (Fig. 6D, Suppl. Fig. 4A) and the 2-thiolated tRNA-Lys^{UUU} levels were also reduced as quantified by APM gel electrophoresis combined with Northern blotting (Fig. 6E). The tRNA-Lys^{UUU} levels were also decreased after incubation of SH-WT cells with SH-SWE cells secretome (Fig. 6F), and no alterations were detected in the expression of tRNA-Glu^{UUC} and tRNA-Gln^{UUG} (Suppl. Fig. 4B, C), and tRNA-Ser^{AGA} (Fig. 6G). To understand if indeed toxic Aβ fibrils trigger ELP3 dysregulation, we incubated SH-WT cells with pre-aggregated $Aβ_{1–42}$ peptides. This resulted in a ~ 50 % decrease in ELP3 abundance in SH-WT cells (Fig. 6H), confirming that it is indeed the exposure to toxic Aβ aggregates that induces a cellular response that triggers ELP3 expression modulation.

3. Discussion

It is now evident that tRNA epitranscriptome dysregulation occurs in a panoply of neurological disorders, as reviewed in [9,47,53]. However, the reports concerning the relevance of the tRNA epitranscriptome in AD are scarce [59], and the role of wobble uridine modifications in neuronal proteotoxic stress generation and their contribution in AD pathogenesis and progression was not yet explored.

Here, we found evidence of dysregulation of tRNA modifying enzyme expression in the brains of AD patients. Our analysis showed that *ELP3* was the most relevant enzyme identified. Besides being dysregulated in both the hippocampus and cortex of AD patients, it was the only tRNA modifying enzyme for which it was possible to establish a negative correlation between its expression and amyloid severity in at least one brain region - the PHG. Previous work has shown that PHG undergoes substantial transcriptomics alterations in AD patients [41] and is associated with early-Aβ deposition and memory loss events [69], supporting a link between the severity of the amyloid pathology and *ELP3* dysregulation. Additionally, from all the dysregulated enzymes identified, *ELP3* was the only one that depicted a negative correlation between

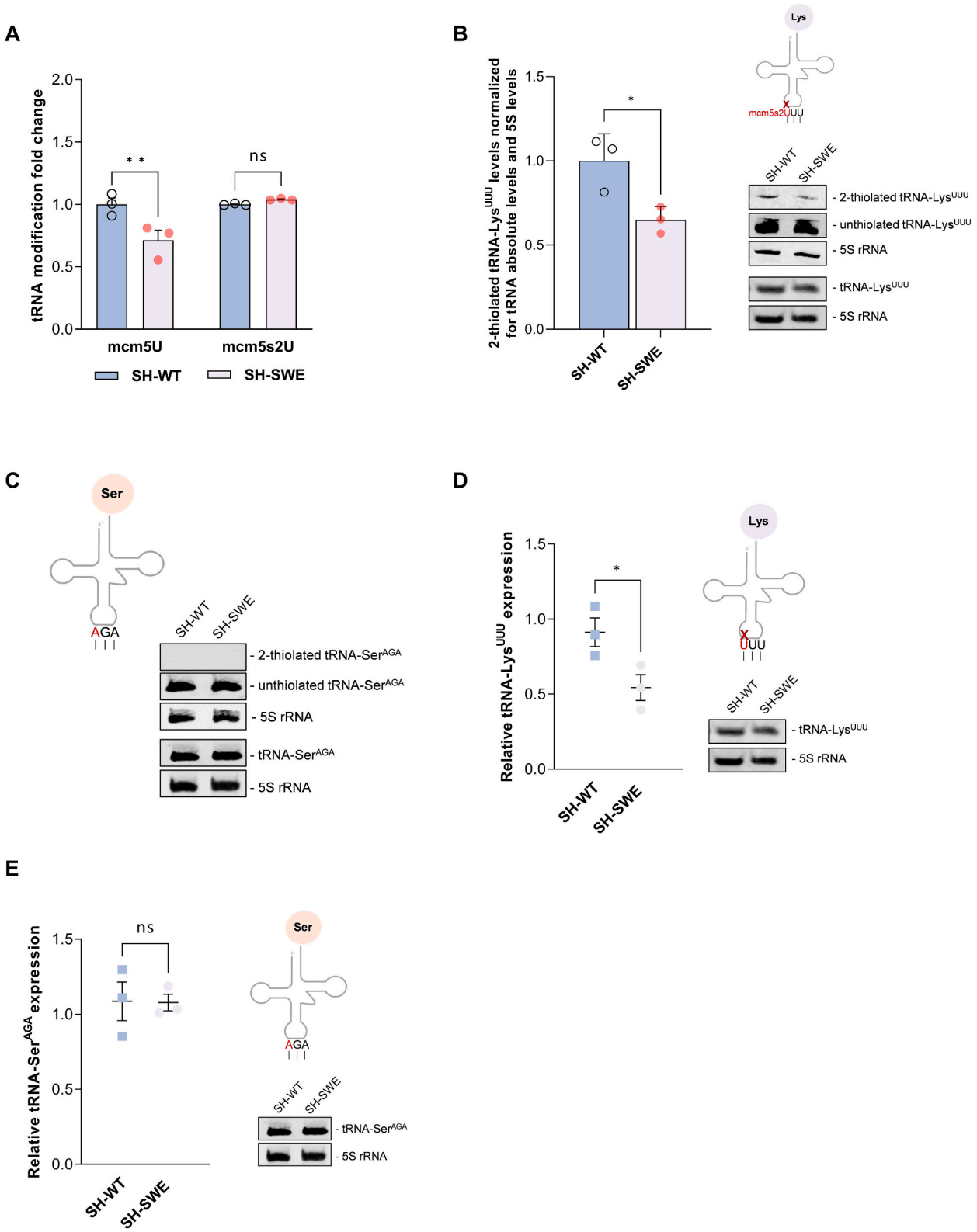

Fig. 4. SH-SWE cells depict tRNA hypomodification and decreased expression levels of tRNA-Lys^{UUU}. A) Quantification of the U34 tRNA modifications in SH-SWE cells by LC/MS-MS. A significant decrease in the level of the ELP3 dependent mcm^{5}U modification was observed in SH-SWE cells compared to SH-WT cells. B) Quantification of 2-thiolated tRNA-Lys^{UUU} levels by Northern blotting. A significant decrease in the abundance of 2-thiolated tRNA-Lys^{UUU} in SH-SWE cells was observed in comparison with SH-WT cells, after normalizing for the total tRNA-Lys^{UUU}. 5S rRNA was used as internal control. C) Quantification of 2-thiolated tRNA-Ser^{AGA} was used as a negative control. No 2-thiolated tRNA-Ser^{AGA} levels were detected in any of the cell lines tested, as expected. 5S rRNA was used as internal control. D) Quantification of mature tRNA-Lys^{UUU} abundance by Northern blotting. Abundance of mature tRNA-Lys^{UUU} was significantly decreased SH-SWE cells, when compared to SH-WT cells. 5S rRNA was used as internal control. E) Quantification of tRNA-Ser^{AGA} abundance by Northern blotting. No significant alterations in the abundance of the total tRNA-Ser^{AGA} was observed between SH-SWE and SH-WT cells. 5S rRNA was used as internal control. Data information: data are expressed as mean with SEM, with a $n = 3$ biological replicates. *p-value <0.05, **p-value <0.01, and non-significant (ns) p-value as assessed by unpaired t-test.

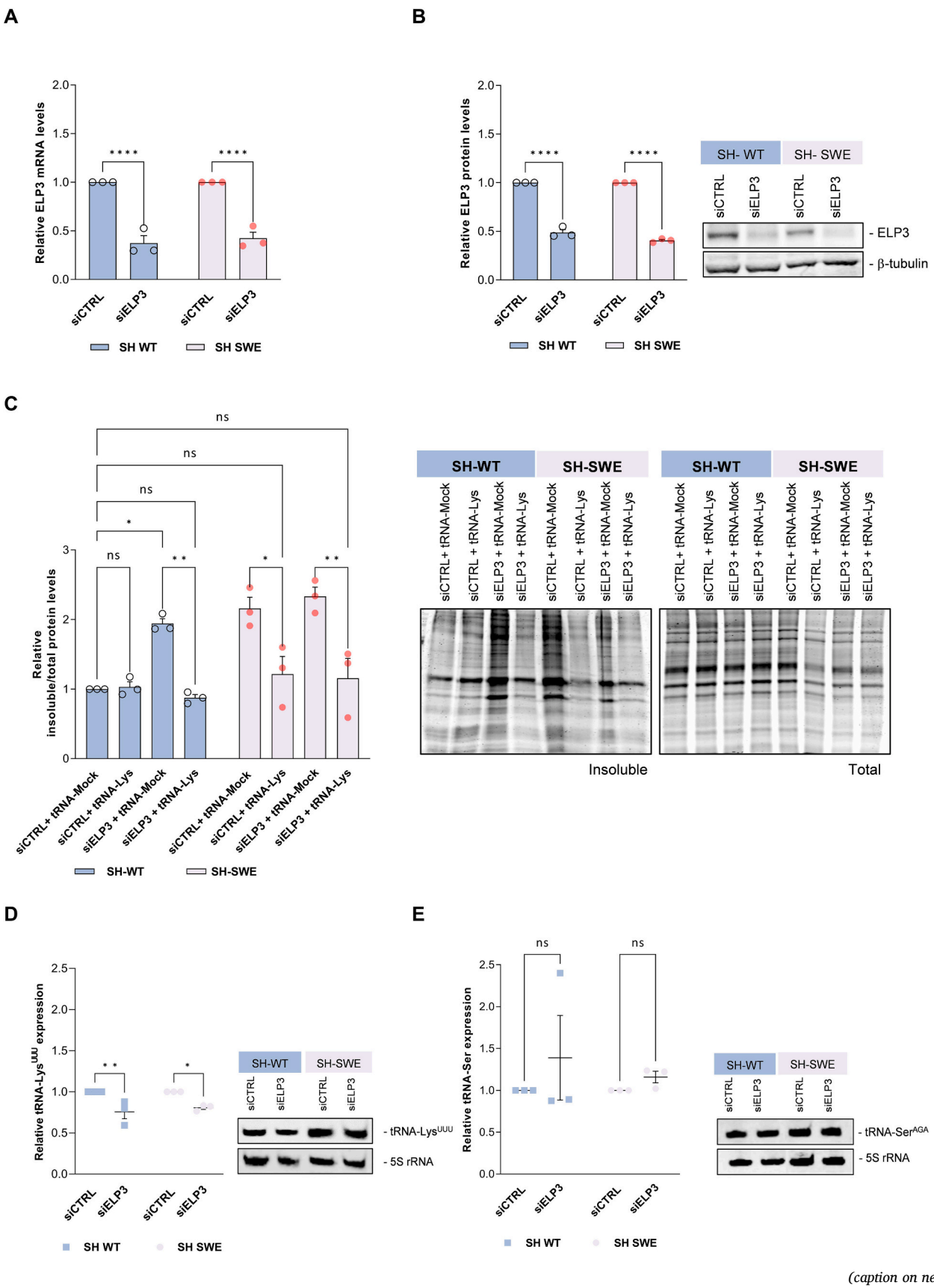

(caption on next page)

Fig. 5. Overexpressing unmodified tRNA-Lys^{UUU} in ELP3-silenced SH-WT and SH-SWE cells restores basal levels of insoluble proteins. A) qPCR analysis of *ELP3* mRNA levels in ELP3 silenced SH-WT and ELP3 silenced SH-SWE cells. A significant decrease in *ELP3* mRNA levels was observed in ELP3-silenced SH-SWE (siELP3) and SH-WT (siELP3) cells when compared to cells transfected with a control siRNA (siCTRL). GAPDH was used as a housekeeping gene. B) Western blot and graphical representation of ELP3 protein levels in ELP3-silenced SH-WT and SH-SWE cells compared to siCTRL transfected cells. A significant decrease in the expression of ELP3 was observed in ELP3- silenced SH-SWE (siELP3) and ELP3-silenced SH-WT (siELP3) cells when compared to control (siCTRL) cells, in both cell lines. β-tubulin was used as an internal control. C) Relative insoluble protein fraction quantifications after transfection of a tRNA-Lys^{UUU} plasmid in ELP3 silenced SH-WT and SH-SWE cells, followed by a representative acrylamide gel staining with blue safe. SH-WT and SH-SWE Cells were co-transfected with the siCTRL and tRNA-Mock plasmid (siCTRL+ tRNA-Mock), siCTRL and tRNA-Lys^{UUU} plasmid (siCTRL+ tRNA-Lys), siRNA against ELP3 and tRNA-Mock plasmid (siELP3 + tRNA-Mock), or siRNA against ELP3 and tRNA-Lys^{UUU} plasmid (siELP3 + tRNA-Lys). Silencing of ELP3 in SH-WT cells resulted in a significant increase in the abundance of insoluble proteins, which was restored upon co-transfection with the tRNA-Lys^{UUU} plasmid. The insoluble protein fraction was also significantly increased in both siCTRL and siELP3-transfected SH-SWE cells, and was restored, in both situations, upon co-transfection with the tRNA-Lys^{UUU} plasmid. D) Quantification of tRNA-Lys^{UUU} abundance by Northern blot after ELP3 silencing in both cell lines. A significant decrease in the abundance of total tRNA-Lys^{UUU} was detected in both SH-SWE and SH-WT ELP3-silenced cells (siELP3) when compared to SH-SWE or SH-WT cells transfected with a control siRNA (siCTRL). E) Quantification of tRNA-Ser^{AGA} abundance by Northern blot after ELP3 silencing in both cell lines. No difference in the abundance of tRNA-Ser^{AGA} was detected in ELP3- silenced SH-WT (siELP3) and ELP3-silenced SH-SWE (siELP3) cells when compared to the respective control cells (siCTRL). Data information: data are expressed as mean with SEM, $n = 3$ biological replicates. *p-value <0.05, **p-value <0.01, and non-significant (ns) p-value as assessed by two-way ANOVA with the Sidak test.

its expression with amyloid and tau pathology, being identified as an early differential expression gene in amyloidogenic murine models.

To validate the relevance of ELP3 in the AD context, we further confirmed that ELP3 mRNA and protein expression was less abundant in the hippocampus of 4 M 5xFAD mice. Different studies reported the existence of extracellular neuronal amyloid deposits and gliosis at this time point that culminate in cognitive deficits, characteristic of the earliest symptomatic stage [16,31]. As expected, and coinciding with ELP3 decreased expression, at this stage we also detected a decrease in the levels of ELP3-dependent tRNA modifications mcm^{5}U and mcm^{5}s^{2}U. Besides these, we also found an increase in the inosine modification. This modification is found at the wobble position of several tRNAs and results from deamination of adenosine to inosine (A-to-I) being catalyzed by adenosine deaminases, including ADAT2 and ADAT3 [52,65]. It is worth mentioning that these two enzymes were found dysregulated in the AD human datasets analyzed by us, but in a compensatory manner. These observations raise additional questions and suggest that this modification can also be relevant in the AD context. It will be important to explore the significance of this apparent tRNA hypermodification for AD pathophysiology in the future.

As we were particularly interested in the implications of ELP3 dysregulation in AD, we further confirmed that the expression of this tRNA modifying enzyme was also decreased in the *in vitro* AD model SH-SWE cell line that is characterized by mutated APP and increased Aβ production and accumulation, in comparison with SH-WT cells [15]. Concomitantly, we found tRNA hypomodifications in the cells bearing the familial AD mutation. Moreover, we observed that SH-SWE cells are characterized by a generalized increase in accumulation of insoluble proteins and decreased protein synthesis. Remarkably, the accumulation of insoluble proteins in SH-SWE cells was reverted by overexpression of an unmodified tRNA-Lys^{UUU}, further reinforcing that ELP3 decreased expression in SH-SWE had a direct impact on tRNA modification levels and proteostasis and that lack of ELP3 triggers the accumulation of insoluble proteins most probably due to tRNA-Lys^{UUU} hypomodification. These findings are in line with what was previously shown in yeast lacking ELP3 [14,51,64], where proteostasis impairments and accumulation of insoluble proteins occur due to tRNA wobble uridine hypomodification. Indeed, the mcm^{5}s^{2}U$_{34}$ modification at tRNA-Lys^{UUU} increases the network of interactions to stabilize codon:anticodon base-pairing, contributing to translation efficiency and fidelity [8,29]. In addition, studies in yeast strains lacking mcm^{5}s^{2}U modifications reveal the occurrence of codon-specific translational pausing [40,64], that increases the accumulation of misfolded proteins and amino acid misincorporations [64]. Since we also have an increase in the eIF2α-P and a slight decrease in the protein synthesis rate, we suggest the integrated stress response (ISR) response is being activated in these cells to assure minimal protein synthesis, as a protective response. These results are consistent with the increase in eIF2α-P found in brains of AD patients and in AD mice models [28,45]. Surprisingly, some studies reported that high levels of eIF2α-P can also increase the expression of β-secretase (BACE1), which accelerates the beta-amyloidogenic pathway involved in the AD pathology [36,44].

Silencing *ELP3* in SH-WT cells caused a similar proteotoxic phenotype as observed in SH-SWE cells, which was rescued by transfection of an unmodified tRNA-Lys^{UUU}. This points towards the potential deleterious effect of ELP3 dysregulation in neuronal proteostasis. However, ELP3 decreased expression detected in the different AD models tested does not explain on its own the proteostasis impairments observed in the disease. This is particularly true in the case of the SH-SWE cells that carry a familial AD mutation that in itself contributes to proteotoxic stress due to accumulation of toxic Aβ forms, as previous studies have reported an increase in Aβ40 and Aβ42 secretion in cell culture media from SH-SWE cells compared to SH-WT [6,24]. Our results led us to question whether ELP3 disruption in AD patients and AD models carrying the APP695 mutation is a cellular attempt to counteract the proteotoxic stress by decreasing translation rate. After incubation of SH-WT cells with SH-SWE secretome, there was a clear and significant decrease in ELP3 abundance. These cells also depicted a decrease in mcm^{5}U$_{34}$ levels, an increase in the insoluble protein fractions and a decrease in protein synthesis rate, fully recapitulating what occurs in SH-SWE cells. Furthermore, incubation of SH-WT cells with pre-aggregated human amyloid 1–42 also led to a decrease in ELP3 expression, recapitulating the ELP3 levels found in SH-SWE cells. These results suggest that cells alter their tRNA epitranscriptome in the presence of amyloid aggregates, possibly to counteract proteotoxic stress, eliciting the ISR that leads to translation attenuation to allow cells to cope with stressful agents. In fact, a reduction in translation levels has been shown to improve the capacity of the proteostasis network to eliminate aberrant proteins and promote health and longevity [25,38]. However, in this pathological state, the decrease in ELP3 and the consequent tRNA hypomodification seems to further contribute to exacerbate the AD phenotype and is not beneficial for the cell. Indeed, AD is characterized by activation of the ISR and reversal of ISR-mediated translation reprogramming results in neuroprotection [11], which demonstrates that ISR activation is not beneficial in AD. One can also not discard that toxic Aβ aggregates may interact directly with ELP3 or other Elongator components, affecting its activity and leading to premature protein degradation. The fact that proteostasis is recovered by tRNA overexpression also indicates that tRNA hypomodification induced by decreased ELP3 expression is not beneficial in the AD context and further highlights the potential of tRNAs to be used as therapeutics to restore proteostasis in diseases characterized by proteotoxic stress, ISR activation or epitranscriptome disruptions.

Altogether, our results indicate that ELP3 expression is dependent on the levels of aberrant proteins and that modulation of ELP3 expression leads to reprogramming of tRNA modifications, with a direct impact on proteostasis and protein synthesis rate. However, it is possible that other tRNA modifying enzymes that are also dysregulated in AD patients may

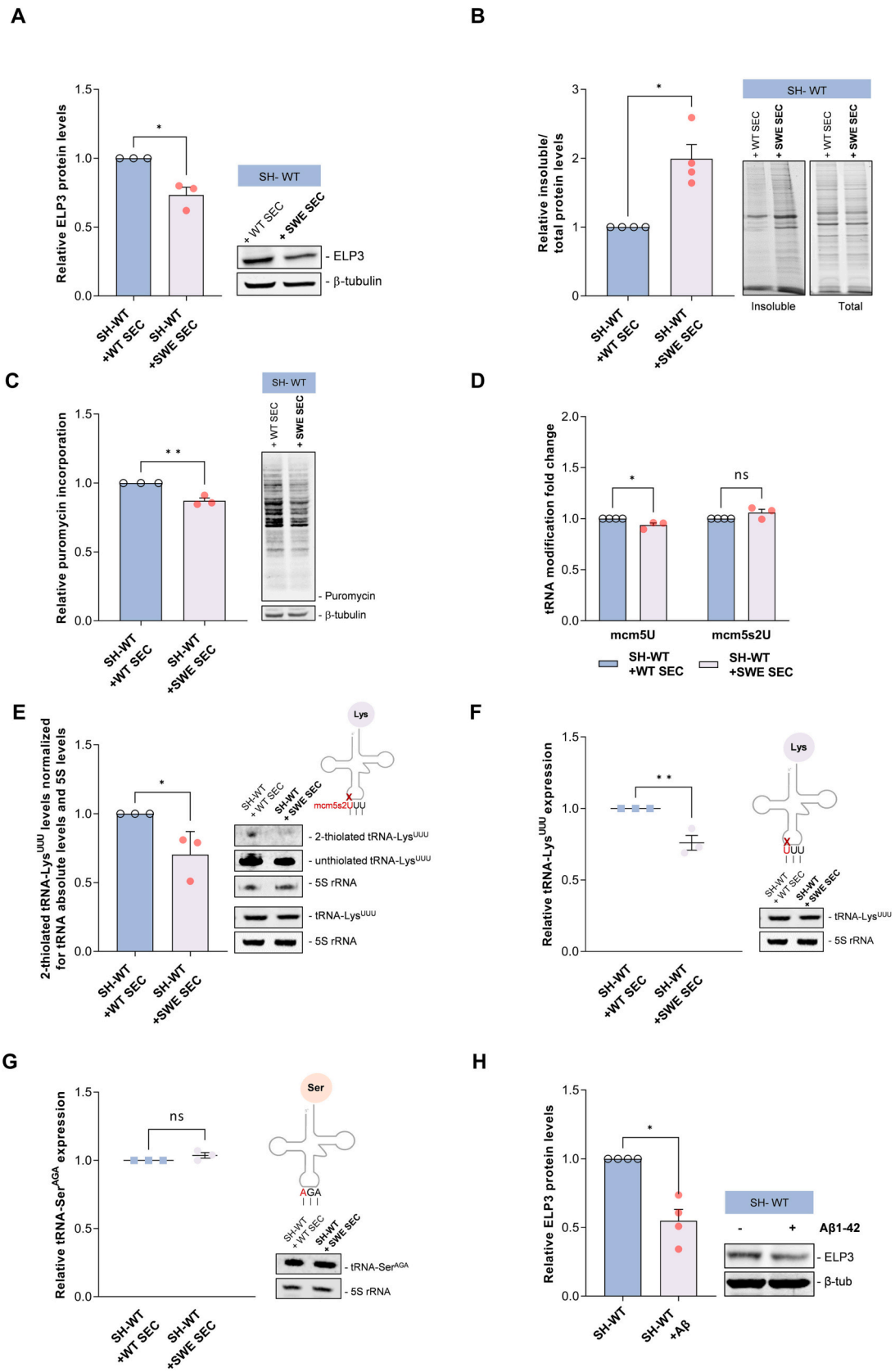

(caption on next page)

Fig. 6. Exposure to the secretome of SH-SWE neuronal cells reduces ELP3 expression and increases the accumulation of insoluble proteins in SH-WT cells. A) Quantification of ELP3 protein expression by Western blotting. A significant decrease in the expression of ELP3 was observed in SH-WT cells incubated with SH-SWE secretome (SH-WT + SWE SEC) when compared to SH-WT cells incubated with their own secretome (SH-WT + WT SEC). β-tubulin was used as an internal control. B) Quantification of the insoluble protein fraction in SH-WT cells after incubation with SH-SWE secretome (SH-WT + SWE SEC), or with SH-WT secretome (SH-WT + WT SEC). A significant increase in the insoluble protein fraction was observed in SH-WT + SWE SEC cells when compared to SH-WT + WT SEC cells. Representative acrylamide gel after blue safe staining is depicted. C) Quantification of protein synthesis rate in SH-WT cells upon incubation with SH-SWE secretome (SH-WT + SWE SEC), or incubation with SH-WT secretome (SH-WT + WT SEC). A significant decrease in protein synthesis rate, identified by a decrease in the incorporation of puromycin, was observed in SH-WT + SWE SEC cells when compared to SH-WT + WT SEC cells. β-tubulin was used as an internal control. D) Quantification of ELP3-dependent U34 tRNA modifications. A significant decrease in the levels mcm5U modification was observed in SH-WT + SWE SEC cells when compared to SH-WT + WT SEC cells, in accordance with the decreased levels of ELP3 expression observed. E) Quantification of 2-thiolated tRNA-Lys^{UUU} abundance. A significant decrease in the abundance of 2-thiolated tRNA-Lys^{UUU} levels occurs in SH-WT + SWE SEC cells, when compared to SH-WT + WT SEC cells, and normalized for the total tRNA-Lys^{UUU} levels. 5S rRNA was used as internal control. F) Quantification of mature tRNA-Lys^{UUU} levels by Northern blotting. A significant decrease in tRNA-Lys^{UUU} abundance is observed after incubation of SH-WT cells with SH-SWE secretome (SH-WT + SWE SEC). 5S rRNA was used as internal control. G) Quantification of tRNA-Ser^{AGA} abundance, used as a control tRNA, by Northern blotting. As expected, no significant alterations in the abundance of mature tRNA-Ser^{AGA} was detected between SH-WT + SWE SEC cells, and SH-WT + WT SEC cells. 5S rRNA was used as internal control. H) Quantification of ELP3 protein expression levels in SH-WT cells incubated with Aβ1–42 peptides (SH-WT + Aβ). A significant decrease in the expression of ELP3 was observed in SH-WT + Aβ cells when compared to SH-WT cells not exposed to synthetic Aβ. β-tubulin was used as an internal control. Data information: data are expressed as mean with SEM, with at least a $n = 3$ biological replicates. *p-value <0.05, **p-value <0.01, and non-significant (ns) p-value as assessed by unpaired t-test.

contribute to the changes in tRNA modification levels in concert with ELP3, even though our data shows that there is no direct correlation with amyloid plaque deposition, for example. Besides ADAT2 and ADAT3 discussed above, this can be particularly relevant for tRNA modifying enzymes such as ALKBH8 that catalyze subsequent modifications to the ones primarily catalyzed by the Elongator complex. In the future, it will be important to further evaluate how amyloid pathology affects the expression of other tRNA modifying enzymes in different amyloidogenic models and if there is a concerted cellular response to the initial ELP3 disruption.

Another important aspect for future consideration is to evaluate if there is a correlation between synaptic density and ELP3 enzymatic activity in AD, and hence any correlation with cognitive function. Previous studies have already shown that indeed ELP3 may be correlated with synaptic defects. For example, it has been previously demonstrated that loss-of-function mutations in the homologue of ELP3 in drosophila led to synaptic defects [61], underscoring the importance of the role of ELP3 in synaptic function and its potential significance in neurodegenerative diseases.

In conclusion, our findings show that the tRNA epitranscriptome is modulated in AD and that this modulation has a direct impact on the proteostasis imbalances observed. Thus, developing strategies to reprogram tRNA epitranscriptome in AD will likely increase the probability of recovering corrupted translation and improve neuronal survival, which should be tested soon in different AD models.

4. Material and methods

4.1. RNA-Seq analysis of post-mortem human brains

To evaluate the differential expression of ELP3 gene between AD cases and controls we accessed the harmonized RNA-seq data from the National Institute on Aging's Accelerating Medicines Partnership in AD (AMP-AD) Consortium and the AD research community and available online at Agora Platform (https://agora.ampadportal.org).

To investigate the association between ELP3 expression levels and amyloid plaque density (number of plaques/mm^2) in the PHG brain region, we used linear regression models (R version 3.6.1).

4.2. 5xFAD mouse model

5xFAD heterozygous (+/−) mice were obtained from the Jackson Laboratory (stock no. 34840-JAX) and express five human familial AD mutations driven by the mouse Thy1 promoter (APPSwFlLon, PSEN1*M146L* L286V]6799Vas). Non-transgenic controls B6 mice were littermates (−/−). To collect brain tissue, mice were anesthetized with 1.2 % 2,2,2-tribromoethanol (Avertin), perfused with ice-cold phosphate buffered saline (PBS), and the brain removed, dissected, and stored at −80 °C until further use. Animal experiments were conducted under the approved Indiana University School of Medicine Institutional Animal Care and Use Committee (IACUC) protocol number 22115.

For qPCR and Western blot analysis, tissue was homogenized in buffer containing 1 % NP-40, 0.5 % sodium deoxycholate, 0.1 % SDS and protease inhibitor cocktail (Sigma Aldrich, #P8340). For RNA extraction, tissue homogenate was mixed in an equal volume of RNA-Bee (Amsbio, CS-104B) and RNA was isolated using phenol-chloroform extraction and a Purelink RNA Mini Kit (Life Technologies, 12183020) with an on-column DNAse Purelink Kit (Life Technologies, 12183025). 1000–500 ng of RNA were converted to cDNA with the High-Capacity RNA-to-cDNA kit (Applied biosystems, 4388950) and qPCR was performed on StepOne Real Time PCR System with Taqman Assays (Life Technologies). The mRNA expression of *Elp3* (Taqman assay Mm00804536_m1) was normalized to *Gapdh* (Taqman assay Mm99999915_g1), and expressed as fold changes relative to controls, using the ΔΔCt method. Protein extracts were obtained by centrifugation of the tissue homogenate 12,000 g at 4 °C for 15 min, and recovery of the supernatant. For Western blot, protein extracts were heated for 5 min at 95 °C, loaded into 4–12 % Bis-Tris gels (Life Technologies), and run at 150 V. Proteins were transferred into immobilon-PPVDF membranes at 400 mA, blocked in 5 % milk in TBS-Tween 0.1 %, and incubated with primary antibodies overnight at 4 °C. All secondary HRP-conjugated antibodies were incubated for 1 h at room temperature. The following primary antibodies were used: Elp3 (Cell Signaling 5728S) and β-actin (Santa Cruz sc-517582).

4.3. Cell culture

SH-SY5Y-WT and SH-SY5Y-appSwe were cultured in Dulbecco's Modified Eagle Medium (DMEM, Gibco, Cat. 11,965,084), supplemented with 10 % of Fetal Bovine Serum (FBS, Sigma-Aldrich, Cat. F1051,) and 2 % of Pen-Strep-Glut (Gibco, Cat. 15,070,063). Both cell lines were a kind gift from Dr. Dora Brites from iMed, Lisbon and were engineered as described in [6].

4.4. siRNA and plasmid transfections

siGenome SMARTpool human siRNA targeting ELP3 (siELP3), and a negative control siRNA (siCTRL) were transfected into the SH-SY5Y-WT and SH-SY5Y-appSWE cells in 24-well plates. Briefly, 10 nM of each siRNA were diluted in Opti-MEM (Gibco, Cat. 31,985,062), followed by addition of 1 μL/well of DharmaFECT 1 (Dharmacon, Cat. T-2001–02). After an incubation of 20 min, 4×10^4 cells/mL were added to each well in DMEM supplemented with 10 % FBS and allowed to growth 72 h at

37 °C in a CO_2 incubator.

For tRNA-Lys^{UUU} overexpression, a DNA fragment of 293 bp, containing the gene encoding the human wild-type tRNA-Lys^{UUU} (Chr11 tRNA#15) and its flanking region, was amplified by PCR and cloned into the modified vector pIRES2-DsRed between ECORI and *Xho*I cloning sites. SH-SY5Y-WT and SH-SY5Y-appSWE cells previously transfected with siCtrl or siELP3 as above were subsequently transfected 48 h after siRNA transfection with 1 μg of plasmid DNA using Lipofectamine2000 (Invitrogen), following manufacturer's instructions. Cells were transfected with an empty vector (tRNA-Mock) or with the plasmid carrying tRNA-Lys^{UUU} gene (tRNA-Lys). After an incubation of 20 min, cells were allowed to grow in DMEM supplemented with 10 % FBS for an additional 24 h at 37 °C in a CO_2 incubator.

4.5. MTT assay for cell viability

Cell viability was assessed using the colorimetric MTT assay (3-(4,5-dimethylthiazol-2-yl)-2,5-diphenyltetrazolium bromide, Sigma-Aldrich). SH-WT and SH-SWE cells were seeded at a density of 6×10^4 cells/mL in a 96-well plate. After 72 h of incubation, the culture medium was replaced with fresh serum-free medium, and 10 μL of MTT solution (5 mg/mL in PBS 1 %) was added to each well. The cells were then incubated for 2 h to allow the MTT reagent to be converted to formazan crystals by metabolically active cells. After the incubation, the MTT solution was carefully removed, and 100 μL of dimethyl sulfoxide (DMSO) was added to each well. The plates were gently shaken for 10 min to ensure complete dissolution of the formazan crystals. The absorbance of each well was measured at a wavelength of 570 nm using a plate reader. All experiments were performed in triplicate to ensure data reliability and reproducibility.

4.6. Total RNA extraction

The total RNA from cell cultures and mouse tissues were extracted using the TRIsure™ (Bioline, Cat. BIO-38033) reagent according to manufacturer's instructions.

In the case of RNA extraction from tissues, 50–100 mg were first homogenized in a glass homogenizer (TissueRuptor II - Qiagen, Cat. 9,001,272).

In the case of RNA extraction from cell lines, cells were detached from microplates, collected in Eppendorf's and centrifuged to obtain cell pellets. The supernatant was discarded, and RNA was extracted from the cellular pellets after addition of 1 mL TRIsure™ to each pellet, following the manufacturer's instructions.

The integrity and quantity of each RNA sample were assessed using a spectrophotometer DeNovix DS-11 and the 4200 TapeStation System or a Bioanalyzer.

4.7. LC-MS/MS of tRNA modification abundance

Transfer RNAs (tRNAs) were isolated from total RNA by size exclusion chromatography (SEC), using an Agilent SEC 300 Å column (Agilent 1100 HPLC system) and ammoniumacetate (0.1 M, pH = 7) as mobile phase at 1 mL/min and 40 °C. The collected tRNAs were vacuum concentrated (Speedvac, Thermo Fisher Scientific) and precipitated at −20 °C overnight after adding 0.1× vol. ammoniumacetate (5 M) and 2.5× vol. ethanol (100 %). After centrifugation at 12000 *g* for 30 min at 4 °C, the resulting tRNA pellets were washed with 70 % ethanol and resuspended in pure water. Following UV quantification at 260 nm (NP80, IMPLEN), 200 ng of the purified tRNAs were digested into nucleosides using benzonase (2 U), phosphodiesterase I (0.2 U), alkaline phosphatase (2 U), Tris pH 8.0 (5 mM), magnesium chloride (1 mM), tetrahydrouridine (5 μg), butylated hydroxytoluene (10 μM) and pentostatin (1 μg) in a final volume of 20 μL. Upon a 2 h incubation at 37 °C, the digested tRNA samples were placed in a 96-well plate, mixed with 10 μL LC-MS buffer and analyzed by LC-MS/MS. Quantification was performed on an Agilent 1290 series HPLC combined with an Agilent 6470 Triple Quadrupole mass spectrometer. Nucleosides were separated using a Synergi Fusion-RP column (Synergi® 2.5 μm Fusion-RP 100 Å, 150 × 2.0 mm, Phenomenex®, Torrance, CA, USA) at a flow rate of 0.35 mL min-1 and a column temperature of 35 °C. Buffer A consisting of 5 mM ammoniumacetate pH 5.3 and buffer B consisting of pure acetonitrile were used as buffers. The gradient for chromatography starts with 100 % buffer A for 1 min, followed by an increase to 10 % buffer B over a period of 4 min. Subsequently buffer B is increased to 40 % over 2 min and maintained for 1 min before switching back to 100 % buffer A over a period of 0.5 min. The column is then re-equilibrated for 2.5 min to reach starting conditions. For MS analysis the nucleosides are ionized using an ESI (electro spray ionization) source (Agilent Jetstream). The instrument was operated in positive ion mode and nucleosides were detected using a dynamic multiple reaction monitoring method.

For absolute quantification, defined concentrations of nucleosides were used as calibration. The calibration solutions ranged from 0.05 pmol to 100 pmol for canonical nucleosides and from 0.0025 pmol to 5 pmol for modified nucleosides. Ψ and D calibrations ranged from 0.01 pmol to 20 pmol. Prior to LC-MS, 1 μL of SILISGen2 (10×, [21]) was co-injected with each calibration and each sample. Data analysis was performed with Agilent's Quantitative Mass Hunter software.

4.8. Total protein extraction and quantification

To obtain total protein extracts, cell pellets obtained after cellular detachment and centrifugation, were resuspended in 100 μL of Empigen Lysis Buffer (ELB - 0.5 % Triton X-100, 50 mM HEPES, 250 mM NaCl, 1 mM DTT, 1 mM NaF, 2 mM EDTA, 1 mM EGTA, 1 mM PMSF, 1 mM Na_3VO_4 supplemented with protease inhibitors (Complete, EDTA-free, Roche, Cat. 11,873,580,001)). Protein extracts were then sonicated for 2 cycles, at a 60 % frequency, for 15 s each, and centrifuged 20 min at 200 *g* at 4 °C. In the end, protein in the supernatants was quantified using Pierce™ Bovine Serum Albumin (BCA) Protein Assay Kit (Thermo Fisher Scientific, Cat. 23,225).

4.9. Insoluble protein extraction

To isolate the insoluble protein fractions, 100 μg of total protein was diluted in 100 μL ELB and centrifuged for 20 min at 16000 *g* at 4 °C. The resulting pellet was solubilized in 80 μL of ELB and 20 μL of NP40 (10 %). Samples were sonicated for 20 s and centrifuged for 20 min at 16000 *g* at 4 °C. The supernatant was removed, and 25 μL of complete ELB and 10 μL of 6× Loading Buffer were added to each pellet. After denaturation at 95 °C for 5 min samples were loaded into a 10 % polyacrylamide gel. Gels containing total protein fractions and insoluble protein fractions were stained with blue safe (NZYTech, Cat. MB15201) for 30 min and revealed with the Odyssey Infrared Imaging system (Licor Biosciences).

4.10. Western blotting

Total protein lysates were immunoblotted onto nitrocellulose membranes and incubated with the following primary antibodies: anti-ELP3 (ThermoFisher, Cat. 702,669, 1:200 dilution), anti-eIF2α (Cell Signaling Cat. 9722, 1:1000 dilution), anti-phosphorylated eIF2α (Abcam, Cat. ab4837, 1:400 dilution), anti-puromycin antibody, clone 12D10 (Sigma-Aldrich, MABE343, 1:10000 dilution), Anti-APP (22C11, 1:1000 dilution), Anti-β Amyloid (D-11 Santacruz, Cat. Sc-374,527, 1:1000) and anti-β-tubulin (Invitrogen Cat. 32–2600 or Proteintech Europe, Cat. 10,094–1-AP, 1:1000 dilution).

4.11. cDNA synthesis and qPCR

cDNA was synthesized using the High-Capacity cDNA Reverse Transcription kit™ (Thermo Fisher Scientific, Cat. 4,388,950),

according to the manufacturer's instructions. The resulting cDNA was used to perform qPCRs using the TaqMan™ Gene Expression Master Mix (Thermo Fisher Scientific, Cat. 4,369,016) according to the user guide directives. GAPDH was used as a housekeeping to normalize gene expression levels. The reaction was carried out in the Applied Biosystems 7500 Real-Time PCR System.

4.12. Northern blotting

For each sample, 5 μg of total RNA was electrophoresed on a 10 % polyacrylamide/urea gel. The RNA was then transferred to a positively charged nylon membrane (Amersham Biosciences, Cat. RPN203B) using a semi-dry blotting system. The RNA was crosslinked to the membrane twice in a Stratalinker equipment at 1200 mJ/cm^2 for 1 min each time. The nylon membranes with the transferred RNA were incubated in a hybridization buffer containing 50× Denhardt's solution, 10 % SDS, 20× SSPE, and miliQ water for 2 h. Following this, non-radioactive probes were added to the hybridization buffer for overnight incubation. The probes were chosen according to their melting temperatures (Tm) with a 5 °C lower temperature:

tRNA-Glu-TTC-1-2: [DY782]5-CCGGGCCACCTGGGTGAAAACCAGGAATCC-3[DY782] (Tm 70 °C); tRNA-Lys-TTT-1-1 [DY782]5-CTGGACCCTCAGATTAAAAGTCTGATGCTC-3[DY782] (Tm 63 °C); tRNA-Gln-TTG-1-1 [DY782]5-TCGGATCGCTGGATTCAAAGTCCAGAGTGC-3 [DY782] (Tm 65 °C), tRNA-Ser-AGA-2-1 5′-[ATT0680] GTCGGCAGGATTCGAACCTGCGCGGGGAGA [ATT0680]-3′ (Tm 70 °C); 5S rRNA 5′-[ATT0680] A TCC AAG TAC TAC CAG GCC C [ATT0680]-3′ (Tm 55 °C).

After the hybridization step, the membranes were washed to remove any unbound probes. Finally, the signal was detected using an Odyssey Infrared Imaging system (Li-cor Biosciences).

4.12.1. APM-northern blotting analysis

The APM-Northern blotting analysis was conducted to evaluate the thiolation status of tRNAs. The APM gels were prepared as three-layer gels to improve separation resolution during electrophoresis, as in [26]. Briefly, the bottom Gel Layer consisted of a 10 % polyacrylamide gel containing 8 M urea without APM. The Middle Gel Layer consisted of a 10 % polyacrylamide gel containing 8 M urea with 100 μg/mL of APM (obtained from an APM stock concentration of 1 mg/mL in formamide). The Top Gel Layer consisted of a 10 % polyacrylamide gel containing 8 M urea without APM. This layer acts as a sealing gel to prevent APM evaporation during electrophoresis. Following the preparation of the APM gels as three-layer gels, we proceeded with the Northern blotting protocol (as described in Section 4.12.).

4.13. Incubation of SH-WT cells with SH-SWE conditioned medium or with synthetic Aβ1–42

For conditioned medium experiments, SH-WT and SH-SWE cell lines were cultured in complete medium (DMEM supplemented with 10 % FBS and 2 % Pen/strep) for 72 h at 37 °C and 5 % CO_2. Following the incubation period, the culture medium was carefully collected. In parallel, SH-WT cells were plated in 12-well plates at a density of 12 × 10^4 cells/mL. After 24 h of cell plating, the medium in each well was replaced with either the collected WT medium (control group) or SWE medium (experimental group) for an additional 72-h incubation period. After the incubation period, cells were detached, collected into Eppendorf's, and centrifuged to obtain cellular pellets. Protein and RNA isolation for subsequent Western blotting, insoluble protein fraction analysis, Northern blotting and tRNA modification quantification was performed as described above from the cellular pellets.

For the synthetic Aβ1–42 (Genic Bio, Cat. A-42-T1–0) incubation experiment, we performed a dilution in PBS and incubated at 37 °C in an Eppendorf for 24 h to form fibrils. SH-WT cells were cultured for 48 h in 12-well plates and 10 μM of Aβ1–42 was added per well for an additional 24 h in DMEM supplemented with 10 % FBS. After the incubation period, cells were detached, collected into Eppendorf's, and centrifuged to obtain cellular pellets. Subsequent Western blot analysis was performed as described above.

4.14. Statistical analysis

Data are presented as mean with SEM and were analyzed using GraphPad Prism® software (Version 9.0).

5. Structured methods

5.1. Reagents and tools table

Antibodies	Reference or Source	Identifier or Catalog Number
Rabbitanti-ELP3 (8H8L24)	ThermoFisher 1:200 WB	Cat # 702669
Rabbit anti-eIF2α	Abcam 1:1000 WB	Cat # ab26197
Rabbit anti-eIF2α P	Abcam 1:1000 WB	Cat # ab32157
Rabbit anti-beta tubulin	Proteintech Europe 1:1000 WB	Cat # 10094–1-AP
Mouse, anti-puromycin (12D10)	Merck 1:10000 WB	Cat # MABE343
Mouse, anti-APP (22C11)	iBiMED	
Mouse, Anti-β Amyloid (D-11)	Santa Cruz 1:200 WB	Cat # sc-374,527
Mouse, Anti-beta tubulin	Invitrogen 1:1000 WB	Cat # 32–2600
IRDye 680RD Goat Anti-Rabbit	Li-COR Biosciences 1:10,000 WB	Cat # 926–68,071
IRDye 800CW Goat Anti-Mouse	Li-COR Biosciences 1:10,000 WB	Cat # 926–32,280
Goat Anti-Rabbit HRP	Bio-Rad 1:10,000 WB	Cat # 1706515
Goat Anti-Mouse HRP	Santa Cruz 1:10,000 WB	Cat # sc-2064

Funding

This research was funded by the Portuguese Foundation for Science and Technology (FCT), POCH, FEDER, and COMPETE2020, through the grants SFRH/BD/135655/2018, SFRH/BD/146703/2019, POCI-01-0145-FEDER-016630 and POCI-01–0145-FEDER-029843, UIDB/04501/2020, under the scope of the Operational Program "Competitiveness and internationalization", in its FEDER/FNR component, and by Centro 2020 program, Portugal 2020 and European Regional Development Fund through the grant pAGE-Centro-01-0145-FEDER-000003. It was furthermore supported by the European Union thought the Horizon 2020 program: H2020-WIDESPREAD-2020-5 ID-952373. A. R.S. is supported by an individual CEEC auxiliary research contract CEECIND/00284/2018.

Author contributions

Conceptualization, M.P. and A.R.S.; methodology, M.P., D.R.R., M. B., M.M., A.P.T., C.D., K.N., S.K., and A.R.S.; data curation, M.P., M.B., A.P.T., C.D.; writing-original draft preparation, M.P.; writing-review and editing, M.M., S.K. and A.R.S.; visualization, M.P.; supervision, A. R.S.; project administration, A.R.S.; funding acquisition, A.R.S., M.M, and S.K. All authors have read and agreed to the published version of the manuscript.

Declaration of competing interest

The authors declare that they have no conflict of interest.

Data availability

Data will be made available on request.

Acknowledgements

We are grateful to Professor Dora Brites (iMed.ULisbon, Faculty of Pharmacy, PT), for providing the human neuroblastoma cells: SH-SY5Y wild-type (SH-WT) and SH-SY5Y carrying the APP695 Swedish mutation (SH-SWE), to Dr. Mafalda Santos (IMM, University of Lisbon), that kindly provided us the tRNA-Lys^{UUU} cloned into the pIRES2-dsRed plasmid and to Dr. Hélio Albuquerque (University of Aveiro) that synthetized the APM component.

Appendix A. Supplementary data

Supplementary data to this article can be found online at https://doi.org/10.1016/j.bbadis.2023.166857.

References

[1] N.-H. Abbassi, et al., How Elongator acetylates tRNA bases, Int. J. Mol. Sci. 21 (21) (2020) 8209, https://doi.org/10.3390/ijms21218209.
[2] A.M. Alazami, et al., Mutation in ADAT3, encoding adenosine deaminase acting on transfer RNA, causes intellectual disability and strabismus, J. Med. Genet. 50 (7) (2013) 425–430, https://doi.org/10.1136/jmedgenet-2012-101378.
[3] Alzheimer''s disease facts and figures, Alzheimers Dement. 17 (3) (2021) 327–406, https://doi.org/10.1002/alz.12328.
[4] S.L. Anderson, et al., Familial Dysautonomia is caused by mutations of the IKAP gene, Am. J. Hum. Genet. 68 (3) (2001) 753–758, https://doi.org/10.1086/318808.
[5] M.T. Angelova, et al., The emerging field of epitranscriptomics in neurodevelopmental and neuronal disorders, Frontiers in Bioengineering and Biotechnology. (2018), https://doi.org/10.3389/fbioe.2018.00046.
[6] N.D. Belyaev, et al., The transcriptionally active amyloid precursor protein (APP) intracellular domain is preferentially produced from the 695 isoform of APP in a β-secretase-dependent pathway, J. Biol. Chem. 285 (53) (2010) 41443–41454, https://doi.org/10.1074/jbc.M110.141390.
[7] A. Bento-Abreu, et al., Elongator subunit 3 (ELP3) modifies ALS through tRNA modification, Hum. Mol. Genet. 27 (7) (2018) 1276–1289, https://doi.org/10.1093/hmg/ddy043.
[8] G.R. Björk, et al., A conserved modified wobble nucleoside (mcm5s2U) in lysyl-tRNA is required for viability in yeast, Rna 13 (8) (2007) 1245–1255, https://doi.org/10.1261/rna.558707.
[9] S. Blanco, et al., Aberrant methylation of t RNA s links cellular stress to neurodevelopmental disorders, EMBO J. 33 (18) (2014) 2020–2039, https://doi.org/10.15252/embj.201489282.
[10] T. Chujo, K. Tomizawa, Human transfer RNA modopathies: diseases caused by aberrations in transfer RNA modifications, FEBS J. 288 (24) (2021) 7096–7122, https://doi.org/10.1111/febs.15736.
[11] M. Costa-Mattioli, P. Walter, The integrated stress response: from mechanism to disease, Science 368 (6489) (2020), https://doi.org/10.1126/science.aat5314.
[12] B. Davarniya, et al., The role of a novel TRMT1 gene mutation and rare GRM1 gene defect in intellectual disability in two azeri families, PLoS One 10 (8) (2015) 1–13, https://doi.org/10.1371/journal.pone.0129631.
[13] M.A. Deture, D.W. Dickson, The neuropathological diagnosis of Alzheimer's disease, Molecular Neurodegeneration. Molecular Neurodegeneration 14 (1) (2019) 1–18, https://doi.org/10.1186/s13024-019-0333-5.
[14] L. Endres, P.C. Dedon, T.J. Begley, Codon-biased translation can be regulated by wobble-base tRNA modification systems during cellular stress responses, RNA Biol. 12 (6) (2015) 603–614, https://doi.org/10.1080/15476286.2015.1031947.
[15] A. Fernandes, et al., Secretome from SH-SY5Y APPSwe cells trigger time-dependent CHME3 microglia activation phenotypes, ultimately leading to miR-21 exosome shuttling, *Biochimie*. Elsevier B.V 155 (2018) 67–82, https://doi.org/10.1016/j.biochi.2018.05.015.
[16] S. Forner, et al., Systematic phenotyping and characterization of the 5xFAD mouse model of Alzheimer's disease, Scientific Data 8 (1) (2021) 1–16, https://doi.org/10.1038/s41597-021-01054-y.
[17] G. Garcia, et al., Neuronal dynamics and mirna signaling differ between sh-sy5y appswe and psen1 mutant ipsc-derived ad models upon modulation with mir-124 mimic and inhibitor, Cells. (2021), https://doi.org/10.3390/cells10092424.
[18] S.D. Girard, et al., Onset of hippocampus-dependent memory impairments in 5XFAD transgenic mouse model of Alzheimer's disease, Hippocampus 24 (7) (2014) 762–772, https://doi.org/10.1002/hipo.22267.
[19] A.K. Greenwood, et al., Agora: an open platform for exploration of Alzheimer's disease evidence, Alzheimers Dement. 16 (S2) (2020) 46129, https://doi.org/10.1002/alz.046129.
[20] T. Hanada, et al., CLP1 links tRNA metabolism to progressive motor-neuron loss, Nature. (2013), https://doi.org/10.1038/nature11923.
[21] Heiss, M. *et al.* (2021) Quantification of modified nucleosides in the context of NAIL-MS, in, pp. 279–306. doi:https://doi.org/10.1007/978-1-0716-1374-0_18.
[22] G.L. Igloi, Interaction of tRNAs and of phosphorothioate-substituted nucleic acids with an organomercurial. Probing the chemical environment of thiolated residues by affinity electrophoresis, Biochemistry 27 (10) (1988) 3842–3849, https://doi.org/10.1021/bi00410a048.
[23] R. Ishimura, et al., Ribosome stalling induced by mutation of a CNS-specific tRNA causes neurodegeneration, Science. (2014), https://doi.org/10.1126/science.1249749.
[24] A. Jämsä, et al., BACE-1 inhibition prevents the -secretase inhibitor evoked a rise in human neuroblastoma SH-SY5Y cells, J. Biomed. Sci. 18 (1) (2011) 1–9, https://doi.org/10.1186/1423-0127-18-76.
[25] T. Jiménez-Saucedo, J.J. Berlanga, M. Rodríguez-Gabriel, Translational control of gene expression by eIF2 modulates proteostasis and extends lifespan, Aging. Aging (Albany NY) 13 (8) (2021) 10989–11009, https://doi.org/10.18632/AGING.203018.
[26] H. Jin, W. Gassmann, RNA abundance analysis, in: H. Jin, W. Gassmann (Eds.), Methods in Molecular Biology, *Springer*. Totowa, NJ: Humana Press, 2012, pp. 111–120, https://doi.org/10.1007/978-1-61779-839-9.
[27] T. Karlsborn, et al., Familial dysautonomia (FD) patients have reduced levels of the modified wobble nucleoside mcm5s2U in tRNA, *Biochemical and Biophysical Research Communications*. 454 (3) (2014) 441–445, https://doi.org/10.1016/j.bbrc.2014.10.116. Elsevier Inc.
[28] H.-S. Kim, et al., Swedish amyloid precursor protein mutation increases phosphorylation of eIF2α in vitro and in vivo, J. Neurosci. Res. 85 (7) (2007) 1528–1537, https://doi.org/10.1002/jnr.21267.
[29] R. Klassen, et al., Loss of anticodon wobble uridine modifications affects tRNA(Lys) function and protein levels in Saccharomyces cerevisiae, PLoS One 10 (3) (2015), e0119261, https://doi.org/10.1371/journal.pone.0119261.
[30] M. Kojic, et al., Elp2 mutations perturb the epitranscriptome and lead to a complex neurodevelopmental phenotype, Nat. Commun. (2021), https://doi.org/10.1038/s41467-021-22888-5.
[31] V. Landel, et al., Temporal gene profiling of the 5XFAD transgenic mouse model highlights the importance of microglial activation in Alzheimer's disease, Mol. Neurodegener. 9 (1) (2014) 1–18, https://doi.org/10.1186/1750-1326-9-33.
[32] J.W. Lee, et al., Editing-defective tRNA synthetase causes protein misfolding and neurodegeneration, Nature. (2006), https://doi.org/10.1038/nature05096.
[33] S. Lefler, et al., Familial dysautonomia (FD) human embryonic stem cell derived PNS neurons reveal that synaptic vesicular and neuronal transport genes are directly or indirectly affected by IKBKAP downregulation, PLoS One 10 (10) (2015) 1–28, https://doi.org/10.1371/journal.pone.0138807.
[34] V. Lemau de Talancé, et al., A simple synthesis of APM ([p-(N-acrylamino)-phenyl] mercuric chloride), a useful tool for the analysis of thiolated biomolecules, Bioorg. Med. Chem. Lett. 21 (24) (2011) 7265–7267, https://doi.org/10.1016/j.bmcl.2011.10.051.
[35] T. Lin, et al., Destabilization of mutated human PUS3 protein causes intellectual disability, Hum. Mutat. 43 (12) (2022) 2063–2078, https://doi.org/10.1002/humu.24471.
[36] T. Ma, et al., Suppression of eIF2α kinases alleviates Alzheimer's disease–related plasticity and memory deficits, Nat. Neurosci. 16 (9) (2013) 1299–1305, https://doi.org/10.1038/nn.3486.
[37] I. Martin, et al., Ribosomal protein s15 phosphorylation mediates LRRK2 neurodegeneration in parkinson's disease, Cell. (2014), https://doi.org/10.1016/j.cell.2014.01.064.
[38] V.E. Martinez-Miguel, et al., Increased fidelity of protein synthesis extends lifespan, Cell metabolism. Cell Metab 33 (11) (2021) 2288–2300.e12, https://doi.org/10.1016/J.CMET.2021.08.017.
[39] F. Mattioli, et al., Biallelic variants in NSUN6 cause an autosomal recessive neurodevelopmental disorder, *Genetics in Medicine*. The Authors 25 (9) (2023), 100900, https://doi.org/10.1016/j.gim.2023.100900.
[40] D.D. Nedialkova, S.A. Leidel, Optimization of codon translation rates via tRNA modifications maintains proteome integrity, Cell. The Authors 161 (7) (2015) 1606–1618, https://doi.org/10.1016/j.cell.2015.05.022.
[41] R.A. Neff, et al., Molecular subtyping of Alzheimer's disease using RNA sequencing data reveals novel mechanisms and targets, Sci. Adv. 7 (2) (2021) 1–18, https://doi.org/10.1126/sciadv.abb5398.
[42] A. Neueder, RNA-mediated disease mechanisms in neurodegenerative disorders, J. Mol. Biol. (2019), https://doi.org/10.1016/j.jmb.2018.12.012.
[43] H. Oakley, et al., Intraneuronal β-amyloid aggregates, neurodegeneration, and neuron loss in transgenic mice with five familial Alzheimer's disease mutations: potential factors in amyloid plaque formation, J. Neurosci. 26 (40) (2006) 10129–10140, https://doi.org/10.1523/JNEUROSCI.1202-06.2006.
[44] T. O'Connor, et al., Phosphorylation of the translation initiation factor eIF2α increases BACE1 levels and promotes Amyloidogenesis, Neuron 60 (6) (2008) 988–1009, https://doi.org/10.1016/j.neuron.2008.10.047.
[45] M.M. Oliveira, et al., Correction of eIF2-dependent defects in brain protein synthesis, synaptic plasticity, and memory in mouse models of Alzheimer's disease, Sci. Signal. 14 (668) (2021) 1–12, https://doi.org/10.1126/scisignal.abc5429.
[46] T. Pan, Modifications and functional genomics of human transfer RNA, Cell Res. 28 (4) (2018) 395–404, https://doi.org/10.1038/s41422-018-0013-y.
[47] M. Pereira, et al., Impact of tRNA modifications and tRNA-modifying enzymes on proteostasis and human disease, Int. J. Mol. Sci. 19 (12) (2018), https://doi.org/10.3390/ijms19123738.
[48] M. Pereira, et al., M5 U54 tRNA hypomodification by lack of TRMT2A drives the generation of tRNA-derived small RNAs, Int. J. Mol. Sci. (2021), https://doi.org/10.3390/ijms22062941.
[49] M. Pérez, J. Avila, F. Hernández, Propagation of tau via extracellular vesicles, Front. Neurosci. (2019), https://doi.org/10.3389/fnins.2019.00698.
[50] E.M. Phizicky, A.K. Hopper, tRNA biology charges to the front, Genes Dev. 24 (17) (2010) 1832–1860, https://doi.org/10.1101/gad.1956510.

[51] L. Pollo-Oliveira, et al., Loss of elongator-and KEOPS-dependent tRNA modifications leads to severe growth phenotypes and protein aggregation in yeast, Biomolecules 10 (2) (2020), https://doi.org/10.3390/biom10020322.
[52] À. Rafels-Ybern, C.S.O. Attolini, L.R. de Pouplana, Distribution of ADAT-dependent codons in the human transcriptome, Int. J. Mol. Sci. 16 (8) (2015) 17303–17314, https://doi.org/10.3390/ijms160817303.
[53] J. Ramos, D. Fu, The emerging impact of tRNA modifications in the brain and nervous system, *Biochimica et Biophysica Acta, Gene Regulatory Mechanisms*. Elsevier 1862 (3) (2019) 412–428, https://doi.org/10.1016/j.bbagrm.2018.11.007.
[54] M. Reverendo, et al., TRNA mutations that affect decoding fidelity deregulate development and the proteostasis network in zebrafish, RNA Biol. 11 (9) (2014) 1199–1213, https://doi.org/10.4161/rna.32199.
[55] V.A.N. Rezgui, et al., TRNA tKUUU, tQUUG, and tEUUC wobble position modifications fine-tune protein translation by promoting ribosome A-site binding, Proc. Natl. Acad. Sci. U. S. A. 110 (30) (2013) 12289–12294, https://doi.org/10.1073/pnas.1300781110.
[56] M. Sardar Sinha, et al., Alzheimer's disease pathology propagation by exosomes containing toxic amyloid-beta oligomers, Acta Neuropathol. (2018), https://doi.org/10.1007/s00401-018-1868-1.
[57] E.K. Schmidt, et al., SUnSET, a nonradioactive method to monitor protein synthesis, Nat. Methods 6 (4) (2009) 275–277, https://doi.org/10.1038/nmeth.1314.
[58] D.J. Selkoe, J. Hardy, The amyloid hypothesis of Alzheimer's disease at 25 years, EMBO Molecular Medicine. (2016), https://doi.org/10.15252/emmm.201606210.
[59] A.M. Shafik, et al., Dysregulated mitochondrial and cytosolic tRNA m1A methylation in Alzheimer's disease, Hum. Mol. Genet. 31 (10) (2022) 1673–1680, https://doi.org/10.1093/hmg/ddab357.
[60] O. Sheppard, M. Coleman, Alzheimer's disease: Etiology, neuropathology and pathogenesis, in: X. Huang (Ed.), Alzheimer's Disease: Drug Discovery, Exon Publications, 2020, pp. 1–22, https://doi.org/10.36255/exonpublications.alzheimersdisease.2020.ch1.
[61] C.L. Simpson, et al., Variants of the elongator protein 3 (ELP3) gene are associated with motor neuron degeneration, Human Molecular Genetics. Oxford University Press 18 (3) (2009) 472–481, https://doi.org/10.1093/hmg/ddn375.
[62] L.D. Stutzbach, et al., The unfolded protein response is activated in disease-affected brain regions in progressive supranuclear palsy and Alzheimer's disease, Acta Neuropathologica Communications. (2014), https://doi.org/10.1186/2051-5960-1-31.
[63] M. Tao, Z. Wensheng, Establishment of a cellular model for Alzheimer's disease by overexpressing Swedish-type mutated APP695, *3rd international conference on bioinformatics and biomedical engineering, iCBBE 2009*, IEEE 2003 (2009) 1–4, https://doi.org/10.1109/ICBBE.2009.5162794.
[64] J.F. Tavares, et al., tRNA-modifying enzyme mutations induce codon-specific mistranslation and protein aggregation in yeast, RNA Biology. Taylor & Francis 18 (4) (2021) 563–575, https://doi.org/10.1080/15476286.2020.1819671.
[65] A.G. Torres, et al., A-to-I editing on tRNAs: biochemical, biological and evolutionary implications, *FEBS letters*, Federation of European Biochemical Societies 588 (23) (2014) 4279–4286, https://doi.org/10.1016/j.febslet.2014.09.025.
[66] F. Tuorto, R. Parlato, rRNA and tRNA bridges to neuronal homeostasis in health and disease, J. Mol. Biol. (2019), https://doi.org/10.1016/j.jmb.2019.03.004.
[67] A.S. Varanda, et al., Human cells adapt to translational errors by modulating protein synthesis rate and protein turnover, RNA Biol. (2020), https://doi.org/10.1080/15476286.2019.1670039.
[68] R. Vassar, Phosphorylation of the translation initiation factor eIF2alpha increases BACE1 levels and promotes amyloidogenesis, Alzheimers Dement. 5 (4S_Part_3) (2009), https://doi.org/10.1016/j.jalz.2009.05.205.
[69] M. Wang, et al., Integrative network analysis of nineteen brain regions identifies molecular signatures and networks underlying selective regional vulnerability to Alzheimer's disease, Genome Medicine. Genome Medicine 8 (1) (2016) 1–21, https://doi.org/10.1186/s13073-016-0355-3.
[70] M. Wang, et al., The Mount Sinai cohort of large-scale genomic, transcriptomic and proteomic data in Alzheimer's disease, Scientific Data 5 (2018) 1–16, https://doi.org/10.1038/sdata.2018.185.
[71] W. Wu, et al., tRNA-derived fragments in Alzheimer's disease: implications for new disease biomarkers and neuropathological mechanisms, J. Alzheimers Dis. 79 (2) (2021) 793–806, https://doi.org/10.3233/JAD-200917.
[72] M. Yoshida, et al., Rectifier of aberrant mRNA splicing recovers tRNA modification in familial dysautonomia, Proc. Natl. Acad. Sci. (2015), https://doi.org/10.1073/pnas.1415525112.